Journal of Chromatography, 201 (1980) 343–357
Elsevier Scientific Publishing Company, Amsterdam — Printed in The Netherlands

CHROM. 13,122

THERMAL FRACTIONATION BY MOVING-BED ION EXCHANGE: PRINCIPLES AND EXPERIMENTS

MICHEL BAILLY* and DANIEL TONDEUR

Laboratoire des Sciences du Génie Chimique, CNRS-ENSIC, 1 rue Grandville, 54042 Nancy Cedex (France)

SUMMARY

A mixture of ionic solutes may be fractionated by using the effect of temperature on the exchange equilibria of these solutes on an ion-exchange resin. We present here predictions and experimental results for the separation of Ca^{2+} and K^+ in a moving-bed system. It is shown that a simple equilibrium model allows one to calculate the operating regime used in the experiments. Results concerning the ternary system Fe^{3+}–Cu^{2+}–H^+ are presented, as an extension of the binary model.

INTRODUCTION

Fixed-bed sorption techniques such as parametric pumping[12] and cycling zone adsorption[13] are based on the shift with temperature of the equilibrium distribution of solutes between two phases. We have designed a double-column, dual-temperature, moving-bed process, which relies on the same temperature-shift effect, but allows continuous fractionation.

The basic design and operating variables of this process are different from, and more numerous than those of distillation, so that despite the analogies, the methodology of distillation applies only in part. An original method of analysis is therefore introduced, based on the concepts of non-linear equilibrium chromatography, *i.e.*, on a transient approach. This analysis is presented for the example of a strongly non-ideal binary mixture, and tentatively extended to a ternary mixture.

MATERIALS AND METHODS

Fig. 1 shows the flow-sheet of the apparatus. It consists of two superposed columns, maintained at different temperatures. The ion-exchange resin moves down the two columns by gravity as a compact bed, and is recycled to the top by hydraulic transport. At the bottom of each column, a rotating tap ensures the transfer of resin at a well-defined flow-rate, while avoiding back-mixing between columns. The whole operating cycle, described in more detail below, is controlled by a microprocessor.

The resin transfer is cyclic: the lower tap (R_c) rotates periodically during a fixed time. The upper tap (R_w) is servo-controlled by the resin level in the lower

0021-9673/80/0000–0000/$02.25

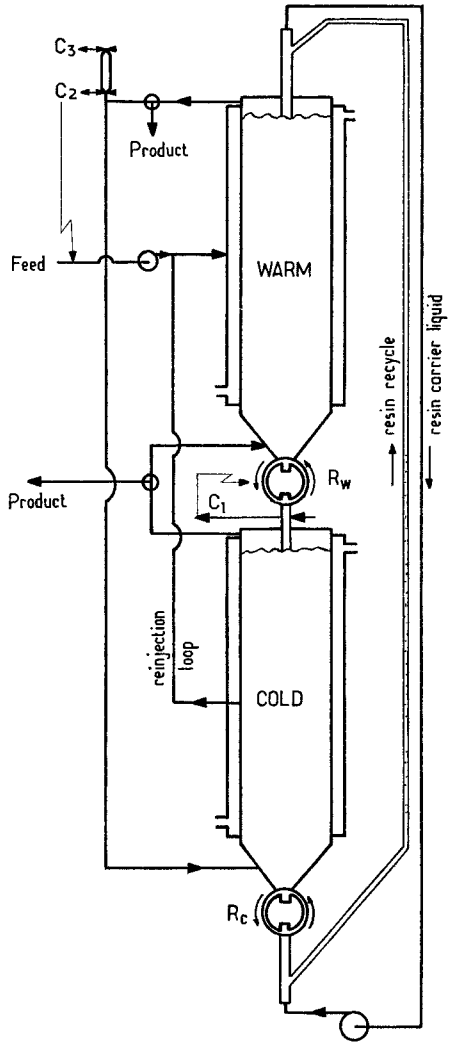

Fig. 1. Experimental apparatus showing moving bed with two serial gravity columns and hydraulic resin recycle. R_i = rotating taps; C_i = control photocells.

column by means of photo-cell detector C_1; each impulse of the latter produces a half-turn of the tap, entailing the transfer of an accurate volume of resin. Counting the number of rotations of the tap R_w per unit time thus gives a good measure of the resin flow-rate, which can be adjusted by changing the period of rotation of the lower tap (R_c). Operating anomalies are also easily detected by this system.

The solution flows counter to the resin in the two columns, *i.e.*, upwards. There are two external solution loops, one which recycles the warm effluent of the upper column to the bottom of the cold column; the other (designated "reinjection loop") withdraws solution from the middle of the cold column, and reinjects it in the middle of the warm column, together with fresh solution to be fractionated.

Periodic withdrawal of products is effected at the top of each column, through three-way electro-valves and a drop-counter which fixes the volume produced at each cycle. Measurement of the time necessary for product collection provides a check for anomalies in solution transfers. Simultaneously, the feed pump is servo-controlled by two photo-cells so as to exactly compensate the withdrawal of products. The timing of its operation provides a check of leakage in the solution circuits.

All the above operations are microprocessor controlled, and the reliability of the apparatus proved sufficient for experiments which required several days to reach the steady state.

Fractionation of a binary mixture, Ca^{2+}–K^+

One of us has shown[1], using an idealized equilibrium model with constant separation-factor isotherm, that the above type of apparatus could theoretically fractionate a binary mixture into two pure products. Here, we illustrate the prediction of the fractionation for a mixture obeying a strongly non-ideal equilibrium.

Characterization of the equilibrium

The ion exchanger is Duolite C-265, a polystyrene sulphonic resin, strongly cross-linked with divinylbenzene. This resin shows relatively important effects of temperature on the exchange equilibria, which are often strongly non-ideal. The exchange isotherms have been carefully determined by batch equilibration of small resin samples of known capacity with known mixtures in thermostated stirred reactors. The experimental results for the Ca^{2+}/K^+ exchange, shown in Fig. 2, have been correlated by the empirical model proposed by Salmon[2]:

$$\ln \frac{y_{Ca}}{x_{Ca}} \left(\frac{x_K}{y_K}\right)^2 = A y_{Ca} [1 + (y_{Ca} - y_K) + (y_{Ca} - y_K)^2 + (y_{Ca} - y_K)^3] + B \tag{1}$$

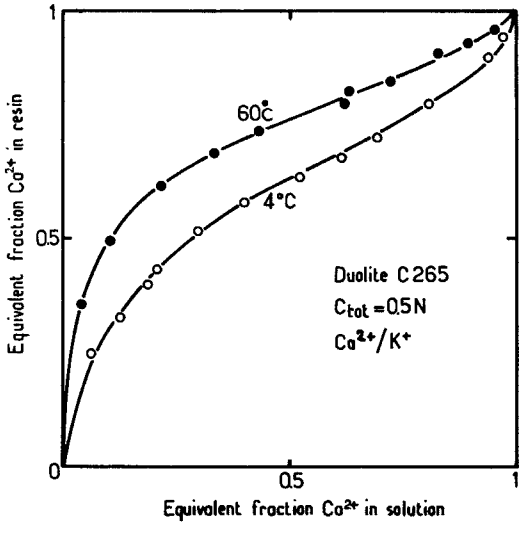

Fig. 2. Equilibrium isotherms for Ca^{2+} and K^+ on Duolite C-265 at 4°C and 60°C. Experimental data are given as circles, the Salmon correlation (eqn. 1) as full lines.

For a total solution normality of 0.5 N, the values of the parameters A and B are -1.17 and 1.87 respectively at 4°C, and -0.8 and 3.11 respectively at 60°C.

Basis of the theoretical approach

The model used is the classical so-called "equilibrium model" used by many authors[3–6] in fixed-bed chromatography, which neglects hydrodynamic dispersion and all resistances to mass transfer. This amounts to considering each column as comprising an infinite number of equilibrium stages. The equilibrium model of chromatography yields the fundamental features of the physical process, summarized below, and which may be transposed to moving-bed operations.

A fixed bed of sorbent, subjected to a step change in inlet compositions, generates two types of composition profiles, when the exchange isotherms are curved. First, dispersive fronts, which spread as they propagate; in these fronts each composition (x, y) propagates at its own velocity, which is related to the local slope of the isotherm by

$$1/T = \mathrm{d}x/\mathrm{d}y \tag{2}$$

where T is the "throughput parameter"

$$T = C(V - Sz\varepsilon)/SzQ \tag{3}$$

and $1/T$ represents the dimensionless velocity of the composition considered. This is the so-called "proportionate pattern" behaviour[4].

Secondly, compressive fronts, which tend to sharpen and to propagate without changing shape (so called "constant-pattern" behaviour). In the equilibrium approach, compressive fronts appear as discontinuities, when the continuous solutions are multivalued and have no physical meaning. Their velocity is given by

$$1/T = \Delta x/\Delta y \tag{4}$$

where Δx and Δy represent the differences in concentration bounding the discontinuity.

The Ca^{2+}/K^{+} exchange isotherm has a sigmoidal shape, which implies that the variation of the inverse of the slope $\mathrm{d}x/\mathrm{d}y$, and hence of $1/T$, changes sign when one goes from $x = 0$ to $x = 1$. The composition profiles generated in a column, as discussed above, may then comprise both dispersive and compressive parts, and are constructed as explained by Tudge[7] or Golden[8] using the continuous solution (eqn. 2) and with the unrealistic multivalued parts replaced by a discontinuity, governed by eqn. 4. A coherence condition must be verified at the junction between the continuous and the discontinuous part: the velocity of the discontinuity must equal the velocity of the composition at the junction. Fig. 3 illustrates these concepts. It shows the effluent history of a column at 60°C (initially Ca^{2+}), fed with a solution of K^{+}. The full line is the experimental result, the dotted line is the unrealistic continuous solution and the interrupted line is obtained by the construction described above.

Transposition to moving beds

Rhee *et al.*[9] have shown how fixed-bed results could be transposed to a single moving bed. We may summarize this transposition in the following way. Consider the composition profile generated by a step change in feed in a fixed bed; suppose the

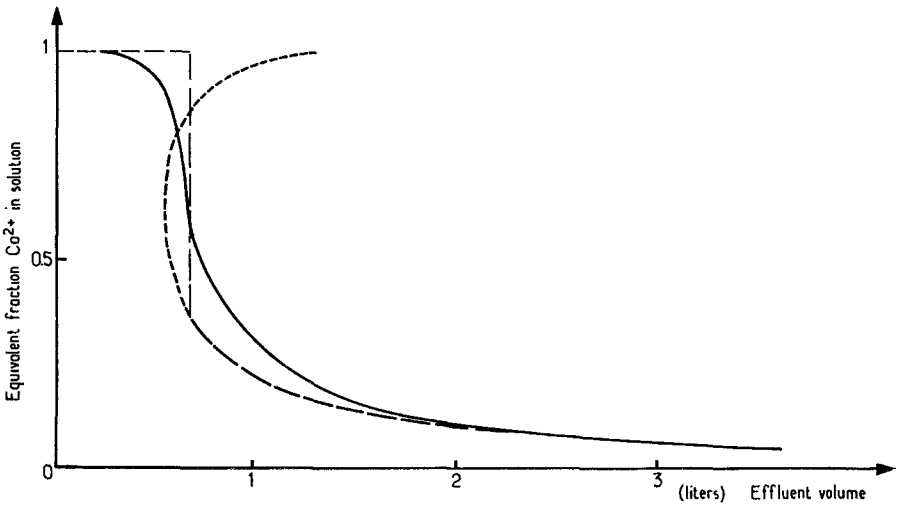

Fig. 3. Elution curve of resin (Ca^{2+}) by K^+ at 60°C. ———, Experimental; – – –, derivative of isotherm; — — —, Golden's model.

adsorbent is put in motion, counter to the solution, at a given flow-rate, and let μ be the flow-rate ratio of resin to solution, expressed in coherent ionic capacity units. A composition, or a discontinuity, of velocity $1/T = \mu$ will then remain fixed with respect to the column, at steady-state. "Faster" compositions or discontinuities will tend to be carried out of the column with the solution, whereas slower ones will be carried away with the resin.

In the present case, we have to consider not only a single column, but a cascade of four coupled sections, each operating with a different value of μ, owing to intermediate withdrawals and injections of solution. In addition, a shift in equilibrium occurs between the warm and the cold columns. To describe the system, we have to solve simultaneously the material-balance equations for the "interfaces", that is the region including the connected extremities of the two columns, where a temperature discontinuity and thus an equilibrium shift exists.

Dual-temperature system: conditions for total separation

A detailed analysis of these couplings has been made[1,10] and we merely recall here pertinent results. We consider the interfaces between the warm and the cold column. Two types of interesting interface behaviour exist, in the sense that they may allow pure products to be obtained.

Fig. 4 shows schematically the concentration profile of Ca^{2+} in the stripping interface. The composition x_{cs} stabilized in the cold column depends on the value, μ_c, of μ imposed in this column. A solution of low calcium content, x_{ws}, is seen to flow from the warm column to the cold column. x_{cs} and x_{ws} are related by:

$$\frac{1}{\mu_c} = \frac{dy_{cs}}{dx_{cs}} = \frac{y_{cs} - y_{ws}}{x_{cs} - x_{ws}} \tag{5}$$

In the enriching interface (Fig. 5), dispersive behaviour is encountered in the warm column instead of the cold column, and a solution rich in Ca^{2+} flows from the cold to the warm column; a relation of the same form as eqn. 5 holds:

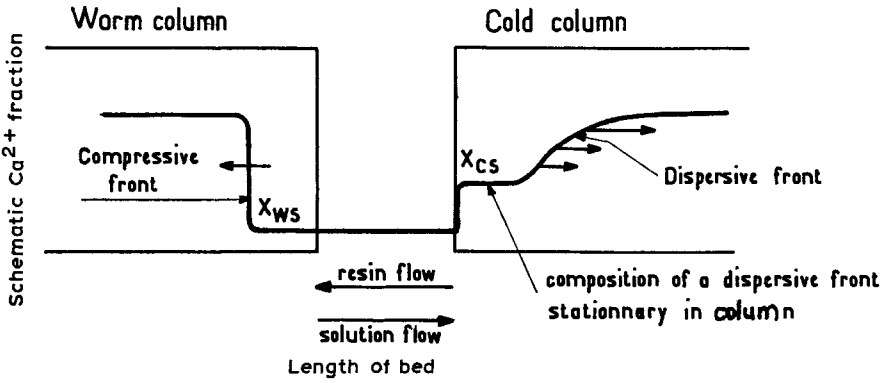

Fig. 4. Schematic calcium composition profile at the stripping interface.

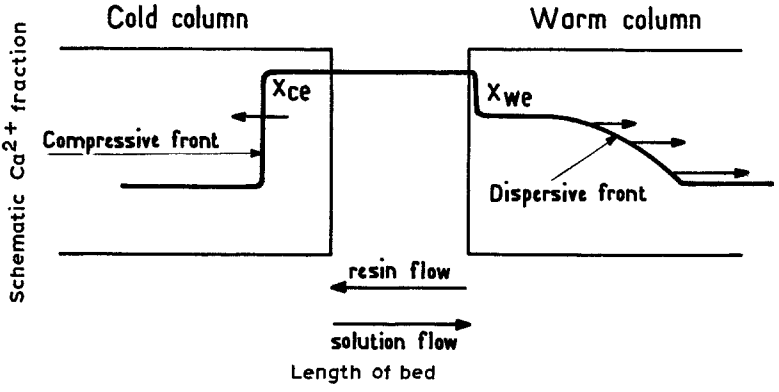

Fig. 5. Schematic calcium composition profile at the enriching interface.

$$\frac{1}{\mu_w} = \frac{dy_{we}}{dx_{we}} = \frac{y_{we} - y_{ce}}{x_{we} - x_{ce}} \tag{6}$$

The conditions required for pure products to be obtained at the interfaces, i.e., $x_{ws} = 0$ (no calcium) at the stripping interface and $x_{ce} = 1$ (no potassium) at the enriching interface, are obtained by substituting these values respectively into eqns. 5 and 6. The solutions obviously imply $x_{cs} = 0$ and $x_{we} = 1$, and the minimal values of $1/\mu$ are obtained by reading the slope of the isotherms at $x = 0$ (cold isotherm) and $x = 1$ (warm isotherm). In the present case, for the stripping interface (cold column) we have

$$\frac{1}{\mu_c} \geqslant \left.\frac{dy}{dx}\right|_{x=0;4°C} = \frac{1}{0.154} \tag{7}$$

and for the enriching interface (warm column):

$$\frac{1}{\mu_w} \geqslant \left.\frac{dy}{dx}\right|_{x=1;60°C} = \frac{1}{1.05} \tag{8}$$

These restrictions on the relative flow-rates of the phases are necessary, but not sufficient to obtain pure products; additional conditions arise from the fact that

the profiles described for both interfaces must be compatible. In the following, we show that this is not so for the present system by studying in more detail the operation of the cold column.

Behaviour of the cold column

Fixed-bed profile. As explained previously, we start from the response of a *fixed* bed of resin (Ca^{2+}, $x_{Ca} = 1$) at 4°C, fed with pure K^+ ($x_{Ca} = 0$). The resulting composition profile is constructed from the isotherm at 4°C (see Fig. 2). Here (Fig. 6) we have plotted directly the equivalent fraction, $x_{Ca}{}^{2+}$, *versus* the reduced velocity, $1/T$, obtained from the inverse slope of the isotherm at point x_{Ca} (eqn. 2). This repre-

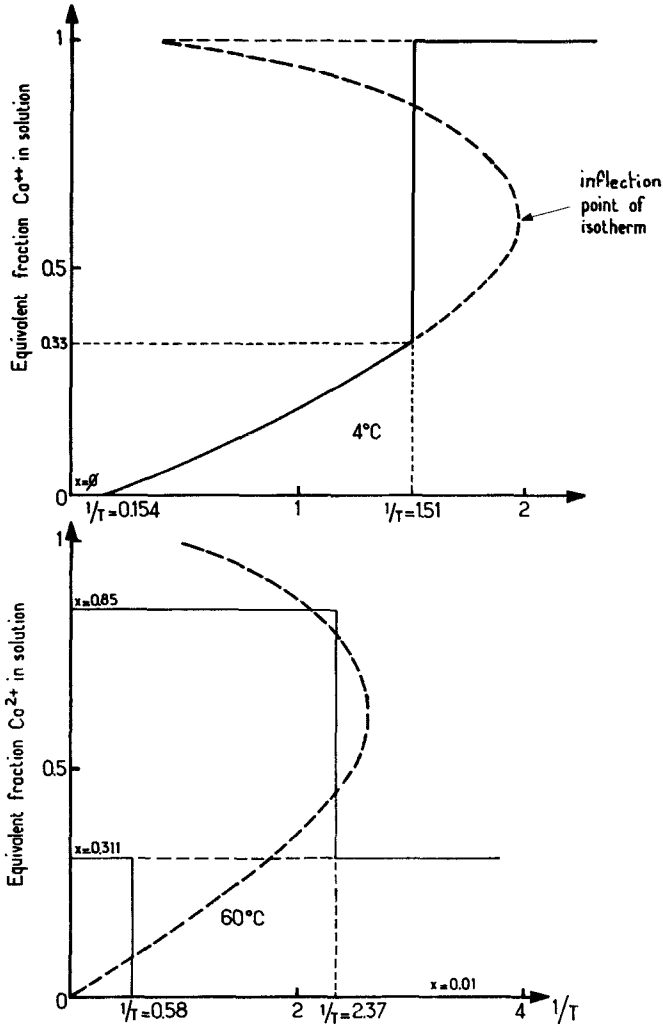

Fig. 6. Theoretical fixed-bed response to feed composition steps. Top: profile in calcium bed fed by potassium solution at 4°C. Bottom: successive profiles in potassium bed fed by calcium solution, ($x = 0.311$ then 0.85) at 60°C. – – –, Fictitious profile obtained from derivation of isotherms; ———, Golden's model.

sentation is a dimensionless concentration profile, and the real profile in the column for any solution throughput is obtained by multiplying the abscissa by the throughput considered, expressed in equivalents. In Fig. 6, we observe that the profile is dispersive for values of x_{Ca} between 0 and 0.33, the corresponding reduced velocities varying between 0.154 and 1.51 respectively. A discontinuity is then encountered between $x_{Ca} = 0.33$ and $x_{Ca} = 1$, the reduced velocity of which is 1.51.

Moving-bed operating regimes. Let us transpose this profile to a moving bed into which the resin is fed (Ca^{2+}, $y_{Ca} = 1$), and the solution feed is pure K^+ ($x_{Ca} = 0$). According to the value of the relative flow-rate μ, three situations may arise.

When $\mu < 0.154$, all concentrations of the profile "move faster" than the resin and are thus carried out with the solution, and the composition $x_{Ca} = 0$ will eventually be established throughout the column. The solution effluent concentration is determined by the material balance accounting for the resin inlet concentration, and a concentration discontinuity thus exists at the solution outlet of the column.

When $0.154 < \mu < 1.51$, a concentration between 0 and 0.33 will be stabilized in the column. For example, when $\mu = 1$, the concentration $x_{Ca} = 0.19$ will be stabilized and tend to be established throughout the column; all larger (hence faster) concentrations will tend to move out with the solution, all smaller (and slower) ones will tend to move out with the resin. The final outlet concentrations will be determined by the material balance around each extremity of the column, where a discontinuity will be established.

When $\mu \geqslant 1.51$ the compressive part of the profile, that is the discontinuity, will be stabilized in the column (for $\mu = 1.51$) or move out with the resin ($\mu > 1.51$), independently of the solution inlet concentration (of course, slower concentrations will also move out with the resin). In either case, the outlet solution concentration is $x_{Ca} = 1$, and the outlet resin concentration results from a material balance around the resin outlet, where a concentration discontinuity is established.

The above analyses of the operating regimes and of the interfaces show that in order to obtain pure products at these interfaces we must satisfy simultaneously the following conditions.

Stabilization of the concentration $x_{Ca} = 0$ at the solution inlet of the cold column, which requires $\mu < 0.154$. This condition is compatible with eqn. 7.

Stabilization of the concentration $x_{Ca} = 1$ at the solution outlet of the same column, which requires $\mu > 1.51$. (This change in μ from one end to the other of the column should be achieved, with the present flow sheet, by suitably adjusting the flow-rate of the sidestream withdrawal; see Fig. 1.) Obviously, the condition $\mu > 1.51$ is incompatible with eqn. 8 which applies to the enriching interface ($\mu_w < 1.05$). This incompatibility is strengthened when product is withdrawn at this interface, since this contributes to increasing μ when going from the cold to the warm column. We conclude that it is impossible to obtain *both* pure products with the flow sheet shown. Nevertheless, one pure product may be obtained and, in the following, we show theoretically and experimentally that good separations are possible.

Achievement of 99% separation

We resume the previous study setting more modest objectives, namely $x_{ws} = 0.01$ and $x_{ce} = 0.99$. Solving numerically eqns. 5 and 6 together with the isotherm eqn. 1, we find the following conditions:

$$\mu_c = 0.605, \qquad x_{cs} = 0.1 \tag{9}$$

$$\mu_w = 2.139, \qquad x_{we} = 0.85 \tag{10}$$

Repeating the analysis of the previous section, we establish that the profiles generated in the cold column are coherent (see Fig. 7).

Coherence of cold-column profiles. A fixed bed of resin equilibrated with $x_{ce} = 0.99$, and receiving a cold feed solution with $x_{cs} = 0.1$, generates a profile comprising a concentration discontinuity between $x = 0.99$ and $x = 0.345$. The velocity of this discontinuity is $1/T = 1.5$. Transposing to moving bed, in order for the discontinuity to move away from the enriching interface, or be stabilized in the cold column, we impose: $\mu_w = 2.139 > \mu_{ce} > 1.5$. This ensures the coherence of the profile in the cold column, solution outlet, side with the enriching interface; on the solution inlet side, letting $\mu_{cs} < 0.605$ ensures the coherence of the profile with the stripping interface where $x = 0.01$. The increase in μ from μ_{cs} to μ_{ce}, as one goes from one end to the other of the cold column, is achieved by adjusting the sidestream withdrawal. For $\mu_{cs} = 0.605$ and $\mu_{ce} = 1.5$, a material balance around the sidestream yields the sidestream composition $x = 0.311$.

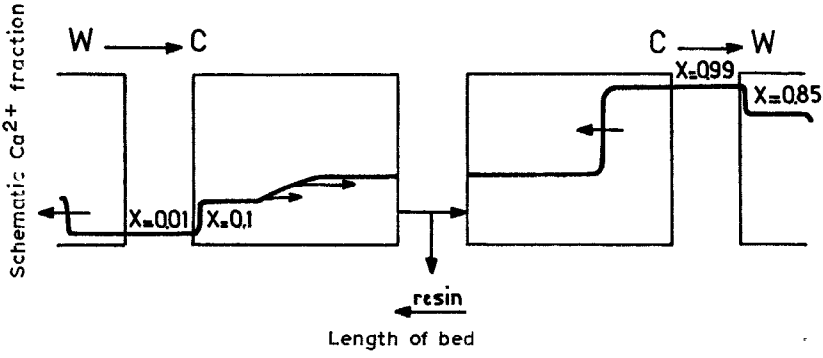

Fig. 7. Schematic coherent composition profile in the cold column.

Coherence of warm-column profiles. Since the sidestream is reinjected between the two warm sections, it must be verified that this does not alter the profiles implied in the warm column by the interfaces assumed above. The material balance around the injection does not furnish an answer. We must perform a perturbation analysis around the injection to prove that it is stable. Thus, we analyse the fronts potentially generated in each section of the warm column by the injection (see Fig. 8). The lower portion of Fig. 6 shows the corresponding fixed-bed profiles obtained from the isotherm at 60°C, and which consist of discontinuities. For the calcium-rich section ($x = 0.85$) the discontinuous front is that which would be obtained by feeding a solution of $x = 0.85$ to a column initially equilibrated at 60°C with $x = 0.311$. The velocity of the discontinuous front is $1/T = 2.37$, larger than $\mu_w = 2.139$ imposed in this section by the enriching interface (condition 10). Therefore the discontinuous front tends to move out of the section on the solution side, and will not perturb the existing profile in the section. A similar argument holds for the calcium-poor section: the

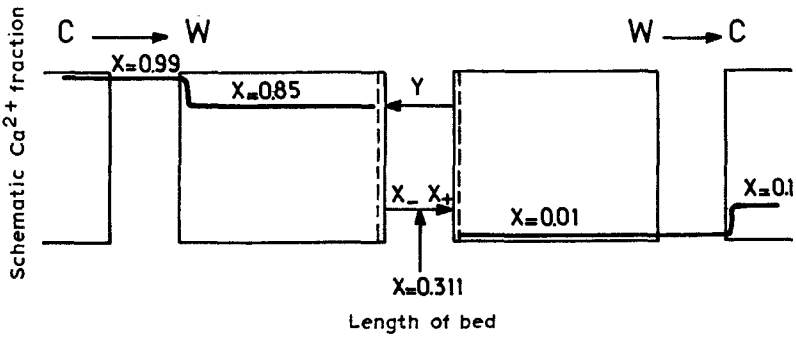

Fig. 8. Schematic coherent composition profile in the warm column.

front obtained by injecting a solution of $x = 0.311$ on the resin equilibrated at 60°C with $x = 0.01$ is a discontinuity of velocity $1/T = 0.577$ (Fig. 6). Since μ in this section must be equal to 0.605 (condition 9), the discontinuous front tends to move out on the resin side, and thus again will not modify the internal profile of the section.

In conclusion, the fronts potentially generated by the reinjected solution in the warm column are "focussed" at the injection and do not alter the profiles assumed in the two sections of the warm column. This ensures the coherence of the entire profile in both columns, while solutions of concentrations $x_{Ca} = 0.01$ and $x_{Ca} = 0.99$ flow respectively at the stripping and the enriching interfaces. We next examine under what conditions these solutions may be withdrawn as products.

Operating with product withdrawal (partial reflux)

We shall show that the profiles analyzed above for "total reflux" operation can be maintained, while a part of the solutions flowing at the interfaces is withdrawn as products, this withdrawal being compensated by feeding fresh solution into the warm column, together with the reinjection. When this is done, in each section of the apparatus a different value of the relative flow-rate, μ, prevails. Let us designate the four sections of the apparatus by 1, 2, 3, 4, section 1 being the part of the cold column that receives the effluent solution from the warm column (see Fig. 9). The corresponding values of μ are μ_1, μ_2, μ_3, μ_4. Two of these values are imposed by the interface conditions (relations 7 and 8), corresponding to the dispersive sections: $\mu_3 = 2.139$; $\mu_1 = 0.605$.

On the other hand, we have shown that the fronts potentially generated by the sidestream withdrawal in the cold column and the reinjection in the warm column tend to remain focused at the point of withdrawal or injection. It is possible to increase the solution flow-rate in section 2 (μ_2 decreases), with respect to the total reflux operation, while the focusing still occurs, thus without alteration of the profile. This is achieved practically by reducing the sidestream flow-rate, and the increase in flow-rate in section 2 is compensated by product withdrawal at the enriching interface, so that μ_3 remains unchanged. The maximum flow-rate in section 2, or minimum μ_2, is that which stabilizes the discontinuous front, *i.e.*, $\mu_{2_{min}} = 1.50$. This corresponds to the maximum calcium-rich product, and to the *minimum reflux at the enriching interface*. The material balance around the sidestream under these conditions yields the concentration of this sidestream: $x_{Ca} = 0.179$.

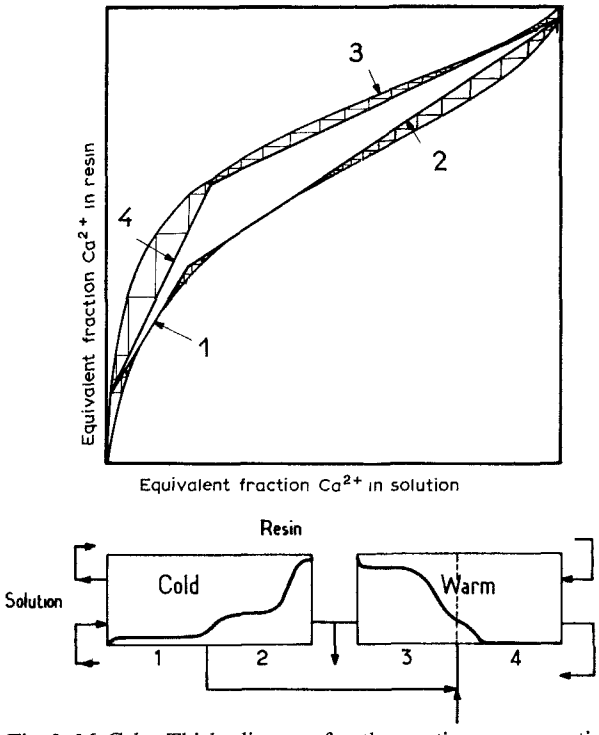

Fig. 9. McCabe–Thiele diagram for the continuous separation (top) and corresponding schematic profile in the bed (bottom).

Similarly, the solution flow-rate can be increased in section 4 to allow withdrawal of calcium-poor product without changing μ_1. This is achieved by injecting fresh feed together with the reinjection in the warm column, at a flow-rate compatible with the focusing of the discontinuous front at the injection point. The latter condition determines the maximum flow-rate in section 4, thus the minimum μ_4, *the minimum reflux for the stripping interface*, and the maximum injection rate. Numerical determination of $\mu_{4\min.}$ must take account of the fresh feed composition, as we shall see in the next section.

Separation of a mixture $x_{Ca} = 0.3$

Maximum product withdrawal. Let us apply the previous results to the determination of the maximal flow-rate for the steady-state separation of a mixture Ca^{2+}–K^+ with $x_{Ca} = 0.3$; the product concentrations desired are $x = 0.99$ and $x = 0.01$.

In addition to the minimum reflux conditions for each interface, determined above, two conditions are imposed by the material balances of the feed and products. Thus the overall material balance gives

$$\frac{1}{\mu_4} - \frac{1}{\mu_3} = \frac{1}{\mu_1} - \frac{1}{\mu_2} + \frac{1}{\mu_F} \tag{11}$$

where μ_F is the dimensionless ratio of the resin capacity flow-rate to the feed flow-rate. The calcium material balance gives

$$0.99\left(\frac{1}{\mu_2}-\frac{1}{\mu_3}\right)+0.01\left(\frac{1}{\mu_4}-\frac{1}{\mu_1}\right)=x_F\frac{1}{\mu_F} \tag{12}$$

where x_F is the calcium fraction in the feed (here $x_F = 0.3$). With μ_1 and μ_3 imposed, eqns. 11 and 12 leave one degree of freedom between the three variables μ_2, μ_4, μ_F. The second of these, μ_4, may be eliminated between the two equations to give:

$$\frac{1}{\mu_2}-\frac{1}{\mu_3}=\frac{x_F-0.01}{\mu_F(0.99-0.01)} \tag{13}$$

A lower limit on μ_F is obtained by letting $\mu_2 = \mu_{2_{min}} = 1.5$ in eqn. 13: $\mu_{F_{min}} = 1.53$.

It must be verified that this flow-rate is compatible with the focusing of the discontinuous fronts at the injection point. We first determine the average composition of the solution injected in the warm column, which results from a mixture of the sidestream from the cold column at a flow-rate expressed by $1/\mu_2 - 1/\mu_3$ and concentration 0.179, and the fresh feed at concentration 0.3 and a flow-rate expressed by $1/\mu_{F_{min}}$. The resulting concentration is $x_I = 0.277$. Using this concentration, we repeat the stability analysis for the warm column. This analysis, not given here, leads to the conclusion that the injection is stable: the discontinuous fronts remain focused at the injection point. There is thus no stronger constraint on $\mu_{F_{min}}$, and the value 1.53 is the minimum, corresponding to the maximum feed input and thus to the maximum product withdrawal. The value of μ_4 is then easily found from eqns. 11 and 12 to be 0.474.

McCabe–Thiele diagram[14]. All the relative flow-rates, μ, are now determined for maximum production; the values $1/\mu$ represent the slopes of the operating line for each section, at steady-state. Fig. 9 shows the McCabe–Thiele diagram corresponding to the values determined above. We see that the concentration of the calcium-rich product is determined by the intersection of operating lines 2 and 3, corresponding to the enriching interface, and similarly for the calcium-poor product. Fig. 9 also shows the classical construction of equilibrium stages between the equilibrium curves and the operating lines explained in basic chemical engineering books[14].

Considering for example operating line 1, we see that a "pinch point" occurs at about $x = 0.1$. This is the concentration of the dispersive profile of Fig. 4, which corresponds to $1/T = 0.605 = \mu_1$. At a "pinch point" an infinite number of equilibrium stages is required to effect an infinitesimal concentration change: the concentration of the pinch point tends to be established along the whole section. At each end of operating line 1 a few stages effect a relatively large concentration change, which corresponds to the discontinuous fronts which are established at each end of section 1.

Similar comments may be made on operating line 3 (pinch point at $x = 0.85$) For operating line 4, a pinch occurs at the lower end, with $x = 0.01$, indicating that this concentration is established over a large part of section 4, near the solution outlet. The rapid change over a few stages shows the existence of a compressive (discontinuous) front.

Performance criterion. Besides the product purity, the performances may be characterized by an overall reflux ratio, defined as the ratio of the flow-rate recycled in the cold column to the feed flow-rate: $R = \mu_F/\mu_1$. The minimum value of R for a feed concentration $x_{Ca} = 0.3$ is $R = 1.53/0.605 \approx 2.5$.

TABLE I

COMPARISON OF EXPERIMENTAL AND THEORETICAL RESULTS AT A REFLUX RATIO OF 10.8

Column: 40 × 3.4 cm. Resin capacity: 2.15 mequiv./cm³ (bed volume); flow-rates: resin, 1.73 cm³/min (bed volume); liquid upflow corresponding to resin downflow, 1.04 cm³/min; sidestream, 7.75 cm³/min; section 2, 3.1 cm³/min; rich product, 0.31 cm³/min (1/10 of cycle time); poor product, 0.7 cm³/min; $C = 0.5\ N$.

	Experiment	*Calculation*
μ_1	0.56	0.605 (dispersive section)
μ_2	1.6	1.5 (minimum)
μ_3	1.94	2.19 (dispersive section)
μ_4	0.54	0.474 (minimum)
R	10.8	2.5 (minimum)
x_{rich}	0.989	0.99
x_{poor}	0.013	0.01

Experimental results

Table I summarizes the results of an experiment with an overall reflux ratio of 10.8, *i.e.*, much higher than the minimum. The operating conditions are close to optimal, and the results are in good agreement with theoretical predictions. The transient composition profile is presented in Fig. 10.

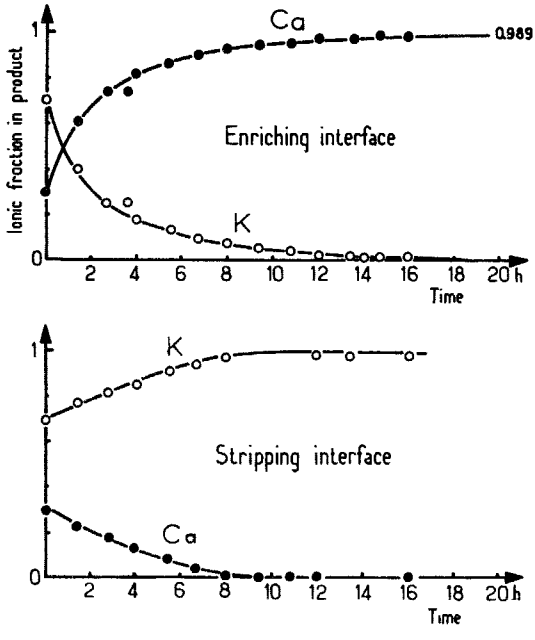

Fig. 10. Composition of the transient production at the stripping and enriching interfaces.

Separation of a ternary mixture, Fe^{3+}–Cu^{2+}–H^+

The principle of the approach outlined above is easily extended to multicomponent systems, although its application is often tedious. Here, we merely present

preliminary experimental results on a ternary system, for which the operating conditions were determined by the present approach.

Ternary equilibrium. We have seen in the binary example that the determination of the operating conditions for a specified separation is strongly dependent on the shape of the isotherm. Therefore, the binary exchanges Fe^{3+}/H^+ and Cu^{2+}/H^+ on Duolite C-265 at 0.5 *N* have been determined as described for Ca^{2+}/K^+. The equilibrium Fe^{3+}/Cu^{2+} cannot be determined directly because of hydroxide precipitation in neutral media. We have used an observation of Brignal *et al.*[11] that the exchange equilibrium of two ions is almost unaffected by the presence of a third one if the latter has a much lower affinity for the resin. We have thus made a series of equilibrations with the ternary mixture, and deduced the binary exchange Fe^{3+}/Cu^{2+} from this. Fig. 11 shows the resulting "pseudo-isotherms" and a noticeable shift of equilibrium with temperature is observed.

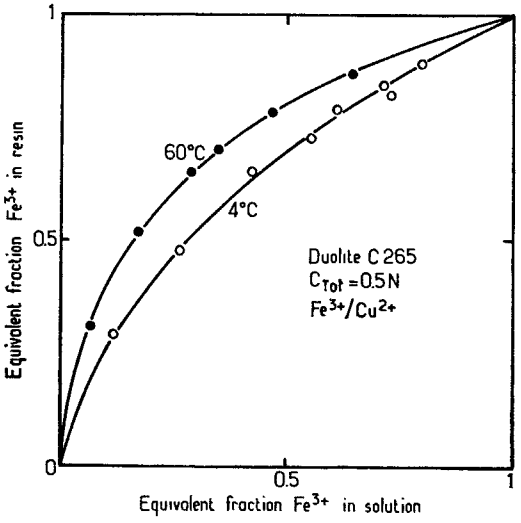

Fig. 11. Equilibrium isotherm for Fe^{3+} and Cu^{2+} on Duolite C-265 at 4°C and 60°C, deduced from ternary Fe^{3+}–Cu^{2+}–H^+ equilibrations.

Experimental results. Table II summarizes the results of an experiment with an overall reflux ratio of around 40. The operating conditions for this experiment are not optimal.

TABLE II

RESULTS OF AN EXPERIMENT AT AN OVERALL FLUX RATIO OF ABOUT 40

	Feed	*Product 1*	*Product 2*
Total normality	0.5		
x_{Fe}	0.10	0.14	0.014
x_{Cu}	0.10	0.0034	0.07
		$\frac{x_{Fe}}{x_{Fe}+x_{Cu}} = 0.975$	$\frac{x_{Cu}}{x_{Fe}+x_{Cu}} = 0.83$

CONCLUSION

Providing the equilibrium isotherms are determined accurately, the equilibrium chromatographic model presented here allows a relatively simple prediction of the maximal performance of the double-column, dual-temperature, moving-bed fractionator. The experimental results obtained indicate that realistic conditions exist for which this idealized approach gives quite acceptable estimates of the performance.

SYMBOLS USED

C	Total solution normality (equiv. per liter)
Q	Total resin capacity (equiv. per liter)
S	Bed section (m^2)
T	Throughput parameter, defined by eqn. 3 (dimensionless)
V	Volume of solution percolated (l)
x_i	Equivalent fraction of species i in solution (equiv. of species/total equiv.) (dimensionless)
y	Equivalent fraction in resin (dimensionless)
z	Abscissa along bed (m)
ε	Bed porosity (dimensionless)
μ	Dimensionless flow-rate ratio: ratio of resin flow expressed in equivalents of exchange capacity/sec to solution flow expressed in equiv./sec

REFERENCES

1 M. Bailly, *Doctorate Thesis*, Nancy, 1977.
2 J. E. Salmon, *Trans. Faraday Soc.*, 65 (1969) 2879.
3 E. Glueckauf, *Disc. Faraday Soc.*, 7 (1949) 12.
4 G. Klein, D. Tondeur and T. Vermeulen, *Ind. Eng. Chem. Fundam.*, 6 (1967) 339.
5 F. Helfferich and G. Klein, *Multicomponent Chromatography*, Marcel Dekker, New York, 1970.
6 H. Rhee, R. Aris and N. R. Amundson, *Phil. Trans. Roy. Soc. London, Ser. A*, 267 (1970) 419.
7 A. P. Tudge, *Can. J. Phys.*, 39 (1961) 1611.
8 F. M. Golden, *Ph.D. Thesis*, University of California, Berkeley, 1963.
9 H. Rhee, R. Aris and N. R. Amundson, *Phil. Trans. Roy. Soc. London, Ser. A*, 269 (1971) 187.
10 M. Bailly and D. Tondeur, *Inst. Chem. Eng. Symp. Ser.*, 54 (1978) 111.
11 W. J. Brignal, A. K. Gupta and M. Streat, *The Theory and Practice of Ion Exchange*, Society of Chemical Industry, London, 1976.
12 R. H. Wilhelm, A. W. Rice and A. R. Bendelius, *Ind. Eng. Chem. Funds.*, 5 (1966) 141.
13 R. L. Pigford, B. Baker and D. E. Blum, *Ind. Eng. Chem. Funds.*, 8 (1969) 848.
14 Treybal, *Mass Transfer Operations*, McGraw-Hill, New York, 1955.